The effects of water on the dielectric properties of aluminum based nanocomposites

Ian L Hosier, Matthew Praeger, Alun S. Vaughan and Steve G Swingler

Abstract—**A series of polyethylene nanocomposites was prepared utilizing aluminum nitride or alumina nano-powders with comparable morphologies. These were subsequently subjected to different conditioning regimes, namely prolonged storage in vacuum, the ambient laboratory environment or in water. The effect of filler loading and conditioning (i.e. water content) on their morphological and dielectric properties was then examined. Measurements indicated that, in the case of aluminum nitride nanocomposites, none of the conditioning regimes led to significant absorption of water and, as such, neither the dielectric properties nor the DC conductivity varied. Conversely, the alumina nanocomposites were prone to the absorption of an appreciable mass of water, which resulted in them displaying a broad dielectric relaxation, which shifted to higher frequencies, and a higher DC electrical conductivity. We ascribe these different effects to the interfacial surface chemistry present in each system and, in particular, the propensity for hydrogen bonding with water molecules diffusing through the host matrix. Technologically, the use of nanocomposites based upon systems such as aluminum nitride, in place of the commonly used metal oxides (alumina, silica, etc.), eliminates variations in dielectric properties due to absorption of environmental water without resorting to the adoption of techniques such as surface functionalization or calcination in an attempt to render nanoparticle surface chemistry hydrophobic.**

Index Terms—**Dielectric spectroscopy, electrical conductivity, nanocomposites, polyethylene, alumina, aluminum nitride.**

I. Introduction

NANOCOMPOSITES, in which a filler with at least one dimension less than 100 nm in size is incorporated into a host matrix, continue to attract considerable interest because of the desirable properties that such systems can exhibit. Indeed, much of the current interest in such systems is often attributed to pioneering work conducted at Toyota in the late 1980s into the development of systems with attractive mechanical properties for use in automotive applications; adding just 4.2 wt. % of montmorillonite clay doubled the modulus, increased the tensile strength by more than 50% and elevated the heat distortion temperature by 100 ºC [1]. From an electrical perspective, the science of nanostructured dielectrics is generally accepted to have begun in 1994, when John Lewis published his seminal paper entitled "Nanometric dielectrics" [2] and, subsequently, such systems have been considered for use in a wide range of electrical applications. These include as high performance insulation systems in power system applications [3], for microelectronic packaging [4], as tailored dielectrics in capacitors [5] and as so-called high k dielectrics for use in applications ranging from organic field-effect transistors to actuators [6].

Several ways of incorporating a nanofiller into a polymeric host are possible [7], including solvent blending using appropriate solvents and surfactants, intercalation through mechanical shearing of the dry nanoparticles within a molten polymeric matrix and the sol-gel method, which involves the formation of nanoparticles directly within the host polymer. Early theoretical considerations led to the development of the "multi-core model" [8], where nanoparticles are envisaged as being surrounded by a diffuse Gouy-Chapman layer of some 10 – 30 nm on a typical 50 nm spherical particle. This is accompanied by an "interaction zone" between the polymeric matrix and the nanoparticles, which is characterized by different properties from either the particle or the matrix. In the case of silica nanocomposites, which are the most commonly reported system in the literature, surface hydroxyl groups are identified as being an important factor in determining the dielectric properties at this interface [7]. A useful review [8] discussed results from other authors and indicated improved breakdown and partial discharge (PD) resistance in well dispersed nanocomposites compared to the host resin. Dielectric spectroscopy results are more varied, with some systems (e.g. silane treated nano-silica) showing reduced dielectric loss whereas other systems (i.e. untreated nano-silica and certain micro-filled systems) gave rise to an additional low frequency dispersion. In another study on electrical treeing [9], tree growth was suppressed, provided the nanocomposite was free of agglomerations, since these can serve as regions of locally high permittivity. Other authors [10] identify good nanoparticle dispersion as being a key pre-requisite for enhanced electrical performance of nanocomposites. Over a wide range of material formulations, improved performance was reported for nanocomposites with

I. L. Hosier and M. Praeger both work as postdoctoral researchers within the Tony Davies High Voltage Laboratory (e-mail: ilh@ecs.soton.ac.uk; mattp@soton.ac.uk).
A. S. Vaughan is currently the head of the Electronics and Electrical Engineering group at the University of Southampton (E-mail: asv@ecs.soton.ac.uk).
S. G. Swingler (retired) was formally a Professor in the Electronics and Electrical Engineering group (E-mail: s. g. swingler@soton.ac.uk)

a low filler loading (< 2 %), but reduced performance thereafter being attributed to particle aggregation. In contrast, the addition of a micro-filler always led to detrimental effects, notably a marked reduction in breakdown strength [11, 12].

Whilst the bulk of the available literature focusses on nanocomposites employing silica, there is a much smaller but significant body of literature concerning alumina-based nanocomposites. Significant improvements in thermal conductivity could be achieved in epoxy systems with high filler loading levels [13]. AC breakdown in epoxy/alumina nanocomposites was also studied [14] and a useful increase in both thermal conductivity and AC breakdown strength was reported for a 5 wt. % filler loading compared to the unfilled epoxy. However, the breakdown strength was reduced at higher filler loading levels. Another study [15] considered the morphology and mechanical properties of epoxy/alumina nanocomposites and demonstrated that probe sonication was an effective way to remove aggregates in the nano-powder. AC breakdown strength was considered [16] and, again, a 5 % filler loading provided enhanced performance but higher filler loadings had detrimental effects. Similar results were reported elsewhere [17]; in a study comparing alumina to silica nanocomposites utilizing epoxy resin as the matrix, 8 % filler was found to be optimal.

A critical element of the use of material systems in real-world applications concerns the effect of exposure to ambient conditions and, in this regard, the influence of water is particularly relevant. Indeed, in the area of adhesives, water effects have been studied by dielectric spectroscopy and it has been shown how water can tend to accumulate at interfaces where local constraints markedly affect its dynamics [18]. Comrie et al. [19], for example, report a correlation between changes in the mechanical strength of adhesive joints and variation in the observed dielectric spectrum. Free, liquid water is characterized by a dielectric relaxation process at about 9.6 GHz [20], but the presence of local interactions can dramatically affect this. Lau et al. [21] reported on the dielectric response of nanosilica/polyethylene systems and showed that water accumulates at nanofiller surfaces to an extend that is dependent upon the nanofiller surface chemistry. The consequence of the local interactions, particularly hydrogen bonding with silanol groups, was markedly retarded dynamics, such that the water relaxation peak was seen to vary from below 1 Hz to above 10^5 Hz, depending on the local, conditions. Elsewhere, ethylene-co-butyl acrylate was used as a matrix together with spherical alumina particles [22]. Under dry conditions, there was little difference in breakdown strength compared to the host material, whereas wet conditioning caused a fall in breakdown strength in the nanocomposite systems - this effect was attributed to water shells surrounding the nanoparticles. In a second publication by the same authors [23], the effect of water conditioning was investigated in detail and, here, it was found that the electrical conductivity of the nanocomposites was higher than that of the unfilled reference material, particularly following storage under wet conditions. Improved thermal conductivity has been reported extensively for relatively high filler loadings (>10 %)

for alumina dispersed within various host polymers [24-26], which could be advantageous in a technological application such as high voltage cables, permitting heat from the conductor core to be extracted more readily, so increasing ratings [27]. However many studies indicate that such high filler loadings are detrimental to dielectric properties [14, 16, 17, 28, 29] such that, in practice, a trade-off between thermal conductivity and dielectric properties may be required.

Only a few papers exist concerning aluminum nitride nanocomposites and these primarily relate to thermal conductivity [30-35]. Thermal conductivity values as high as 4 $W.m^{-1}.K^{-1}$ have been reported in poly(vinylidene fluoride) (PVDF) [30] and epoxy [30, 31] nanocomposites at >50 vol. % filler loading. Values close to 1 $W.m^{-1}.K^{-1}$ were reported in polystyrene systems with 40 vol. % filler loading [32] and in low density polyethylene (LDPE) nanocomposites with ~30 vol. % filler loading [33]. Values of up to 3.3 $W.m^{-1}.K^{-1}$ were reported in poly(methyl methacrylate) (PMMA) nanocomposites containing a 70 vol. % filler loading [34] and, finally, values of up to 0.9 $W.m^{-1}.K^{-1}$ were reported in silicone rubber nanocomposites with a 30 vol. % filler loading [35]. However a recent study [36], in common with the alumina findings, indicates that such high filler loadings are highly detrimental to dielectric performance. Nevertheless the higher intrinsic thermal conductivity of aluminum nitride may make it possible to prepare a nanocomposite with improved thermal conductivity and good dielectric properties using a relatively low filler level [14].

Previously, silica based systems were studied by the authors [37] and it was found that the dielectric properties were highly sensitive to conditioning and several papers indicate that this may also be the case for alumina [22, 23]. Drying the nanocomposites led to electrical properties similar to that of the host polymer, whereas absorbed water always had a detrimental effect. In contrast, silicon nitride nanocomposites [38] absorbed much less water and as a result performed much better in dielectric tests after long term storage under ambient conditions. However, good particle dispersion led to the formation of a percolating network which had a detrimental effect on dielectric properties. Evidently, nanoparticle dispersion, nanoparticle surface chemistry and consequent interfacial interactions with water from the environment are important in determining dielectric characteristics.

The investigation reported here was undertaken with two specific objectives in mind:

(a) To contrast the dielectric behavior of nanocomposites based upon alumina, where the surface chemistry is dominated by hydroxyl groups, with that of systems based upon aluminum nitride, which has a very different surface chemistry. Although this might appear merely to repeat our previous work on silicon based systems [38], the propensity of silicon nitride to form an oxynitride surface layer renders its surface chemistry very different from that of aluminum nitride.

(b) To consider, further, the effects of absorbed water on dielectric characteristics and, consequently, to evaluate the technological utility of nanocomposites based upon alumina

and aluminium nitride in terms of their ability to withstand environmental exposure – a critical technological requirement in numerous electrical applications.

II. EXPERIMENTAL

A. Materials and blending

Commercial alumina (Al_2O_3) and aluminum nitride (AlN) grades were obtained from Sigma Aldrich and were chosen from those that were available to be as comparable as possible (Al_2O_3 – quoted particle size < 50 nm; AlN – quoted particle size ≤ 100 nm). These were used as supplied. A blend of 20 wt. % high density polyethylene (HDPE, BP Chemicals Rigidex HD5813EA) with 80 wt. % low density polyethylene (LDPE, ExxonMobil Chemicals LD100BW) was prepared by melt mixing [21, 38] and was used as the polymeric host.

To improve particle dispersion, a modified solvent blending method was used; 5 g of the polymer blend was dissolved in 50 ml of boiling xylene. Concurrently, either 0.25 or 0.5g of the required nanopowder was dispersed in 10 ml of isopropyl alcohol (IPA). This mixture was sonicated for a total of 10 min using a Hielscher UP200S probe sonicator, with stirring halfway through. The xylene/polymer solution was removed from the heat and allowed to gel slightly and the nanopowder/IPA solution was immediately added. Vigorous stirring was maintained until the mixture had thickened to a waxy solid, this material was then vacuum dried and pressed into sheets. A total of five blends, two using alumina, two using aluminum nitride and an unfilled control, were prepared, as indicated in Table I.

B. Sample preparation and conditioning

Samples were melt pressed into 0.2 mm and 0.1 mm thickness sheets using a hydraulic press maintained at 180 °C. All samples were crystallized from the melt in an oil bath maintained at 115 °C for 1 h prior to quenching in water [21, 37, 38]. Specimens were then conditioned to vary their water content as follows. "Ambient" samples were maintained under ambient conditions in an air conditioned environment (19 ± 2 °C, 55 - 80 % RH) for at least 14 days prior to testing; "dry" samples were vacuum dried at room temperature for periods of up to 14 days; "wet" samples were immersed in water for periods of up to 14 days. These latter two batches of samples will subsequently be referred to as Dry N d and Wet N d, where N d represents the number of days of conditioning in vacuum or water respectively. The mass of each sample was recorded during conditioning to an accuracy of ±0.0001 g (i.e. ± 0.02 % on typical 0.5 g samples).

C. Characterization

Nano-powder for energy dispersive X-ray spectroscopy (EDS) was mounted using double sided carbon tape onto carbon scanning electron microscopy (SEM) stubs. These specimens were then examined in a Philips XL30 environmental SEM operated at 10 kV and four spectra were taken from 50 μm^2 areas. The Kα peaks of Si (1.74 keV), O (0.52 keV), N (0.39 keV) and C (0.28 keV) were recorded and peak area analysis was used to estimate the elemental concentrations.

Thermogravimetric analysis (TGA) was performed using a Perkin Elmer Pyris 1 TGA by heating 5 mg samples at a rate of 20 $K.min^{-1}$ in air.

Samples for SEM were etched for 4 h in a solution of 1 % potassium permanganate in an acid mixture (5:2:1 of sulfuric, phosphoric acids and water respectively) following published procedures [39]. Samples were mounted onto aluminum SEM stubs, gold coated and were then examined at 15 kV in a JEOL JSM6500F high resolution field emission gun SEM.

Differential scanning calorimetry (DSC) was performed using a Perkin Elmer DSC-7, which was calibrated using high purity indium. Melting scans were obtained through heating at 10 $K.min^{-1}$, while the crystallization behavior was determined by cooling at 5 $K.min^{-1}$.

Dielectric spectroscopy was performed on 0.2 mm thick samples incorporating gold coated electrodes, using a parallel plate test cell with a guard ring (inner electrode 30 mm diameter). Measurements of permittivity and dielectric loss were performed using a Solartron 1296 dielectric interface linked to a Schlumberger SI 1260 impedance-gain-phase analyzer. A 1 V_{rms} AC signal was applied over a frequency range from 0.1 Hz to 1 MHz averaging over 10 cycles and all measurements were performed at room temperature.

Measurements of electrical conductivity were performed at room temperature on the same (coated) samples placed between opposing 20 mm diameter polished gold electrodes. A stepped voltage (100 V_{dc} to 6 kV in steps of 100 V) was applied, waiting 10 s before measuring the current, to allow capacitive currents to dissipate.

III. RESULTS

A. Composition and morphology

Table II shows the chemical composition of the nanofillers (uncertainty ± 3 %). The Al_2O_3 contains close to the expected 2:3 ratio of aluminum to oxygen and negligible nitrogen. AlN contains somewhat more than the expected 1:1 ratio of aluminum to nitrogen, which is unexpected. In silicon nitride, an excess of oxygen was detected [38], which was attributed to the formation of an oxynitride layer; this layer is not expected to form in aluminum nitride at room temperature [40] and accordingly, little oxygen was detected in this system

TABLE I
BLENDS USED IN THESE INVESTIGATIONS

Blend	Base resin	Nanofiller used
Control	20 wt. % HDPE / 80 wt. % LDPE	-
AlN05	20 wt. % HDPE / 80 wt. % LDPE	5 wt. % AlN
AlN10	20 wt. % HDPE / 80 wt. % LDPE	10 wt. % AlN
AlO05	20 wt. % HDPE / 80 wt. % LDPE	5 wt. % Al_2O_3
AlO10	20 wt. % HDPE / 80 wt. % LDPE	10 wt. % Al_2O_3

TABLE II
RESULTS FROM EDX ANALYSIS OF THE NANOFILLERS

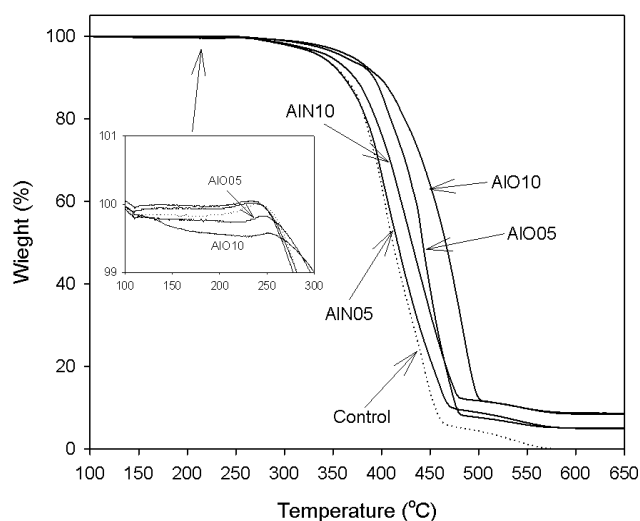| Powder	Aluminum (wt. %)	Oxygen (wt. %)	Nitrogen (wt. %)
Alumina	43	57	-
Aluminum nitride	58	1	41

Fig. 1. TGA curves obtained from the five nanocomposites following ambient conditioning.

(Table II).

The TGA curves shown in Fig. 1 indicate that the onset of degradation occurs close to 300 °C. While neither of the aluminum nitride-based composites loses any significant mass up to 300 °C, AlO10 loses ~0.4 % of its initial mass, with AlO05 losing somewhat less (arrowed, inset Fig. 1). Since

these results may be associated with the loss of absorbed water, two additional samples of AlO10, which had undergone Wet 7 d and Dry 7 d conditioning were also analyzed. Whilst the dry sample lost <0.2 % of its mass when heated to 300 °C, the wet sample lost appreciably more mass (0.7 %) than the ambient sample discussed above, confirming that the alumina-based systems do indeed absorb some water on exposure to the laboratory environment and more when wet conditioned.

At higher temperatures the host polymer starts to degrade; the unfilled control sample loses 50 % of its initial mass at 410 °C whilst, in AlN05 and AlN10, this point is displaced to higher temperatures, indicating improved thermal stability. The 50 % mass loss point is elevated yet further in AlO05 and AlO10, indicating that alumina has a greater influence on thermal stability. Similar improvements in thermal stability in both types of nanocomposites, within polyethylene hosts, have been reported elsewhere [41, 42] and are generally attributed to the propensity of the filler to promote the formation of char. The final residue (i.e. filler) contents measured at 570 °C (where the polymer is assumed completely to have degraded) are within 1 % of the expected values.

Representative SEM micrographs obtained from all the nanocomposite systems are shown in Figs. 2 and 3; the morphology of the control sample has been discussed in detail elsewhere [21, 37, 38] and, being identical to that shown Fig. 2a, albeit that the 4 AlN inclusions would not be present, is
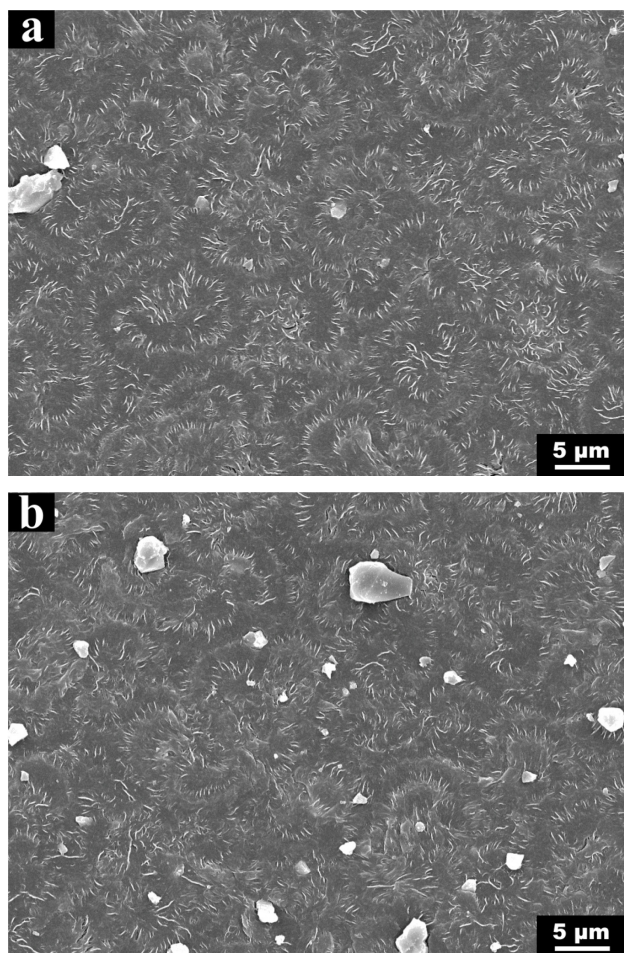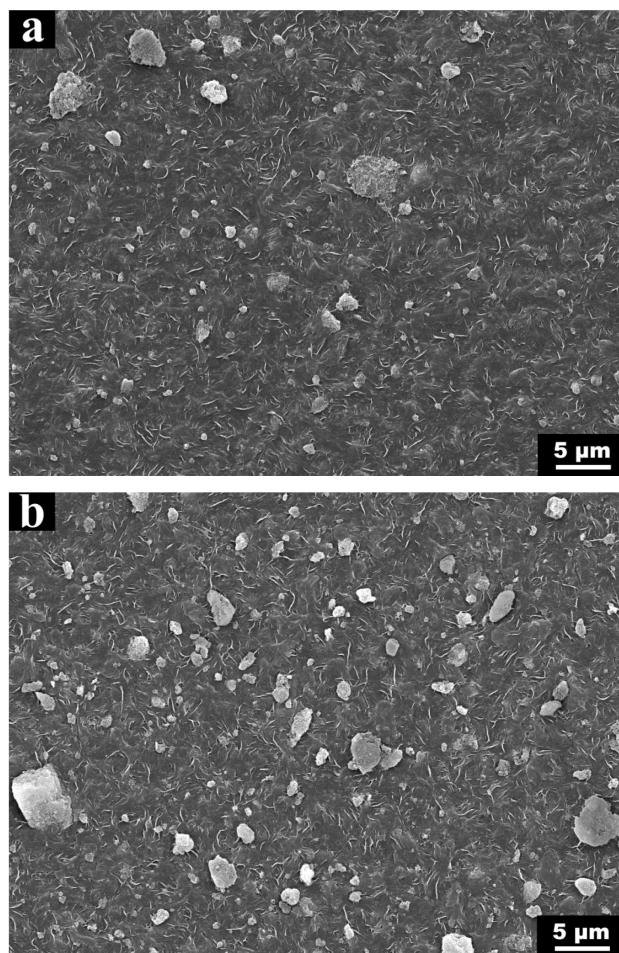

Fig. 2. SEM micrographs (a) AlN05, (c) AlN10.

Fig. 3. SEM micrographs of (a) AlO05, (c) AlO10.

not shown here for brevity. The two aluminum nitride composites (Fig. 2) exhibit an equivalent underlying spherulitic texture to the control sample but, in addition, contain a broad distribution of individual particles ranging from the expected 100 nm right up to 5 μm in size. Even in ALN10 (Fig. 2b) which, as expected, shows a higher density of AlN inclusions, there is no obvious particle aggregation. That is, the primary particles are efficiently dispersed within the host polymer and span the size range given above; that is, the larger inclusions seen here are not the result of agglomeration of smaller entities. In previous reports on aluminum nitride-based nanocomposites, the supplied particles were reported not to be spherical, as here, and a broad distribution of particle sizes ranging from nano- to micrometric size were observed [31-35]. The distribution observed here is therefore consistent with other studies.

The two alumina nanocomposites (Fig. 3) show disrupted spherulitic textures, which are suggestive of enhanced polymer nucleation, and contain Al_2O_3 inclusions ranging in size from ~50 nm to 5 μm. In thermosetting epoxy/alumina systems, both good [14, 16] and poor [17] alumina particle dispersions have been reported, whilst another study using the more relevant thermoplastic host polymer ethylene-co-butyl acrylate [22] indicated very similar aggregated morphologies to those reported here.

The state of nanoparticles within any nanocomposite will depend on both the way in which the constituent components are processed (here, solution processing with sonication) plus the preliminary nanoparticle synthesis route. In the case of AlN, for example, many different routes have been devised, which can result in a wide range of different particle morphologies, as is evident in the above micrographs [43, 44].

Nevertheless, compared to previous work [38], the morphologies of the two types of nanocomposites considered here are much better matched and represent an intermediate level of particle dispersion between silica (poor dispersion, much aggregation) and silicon nitride (good dispersion, little aggregation).
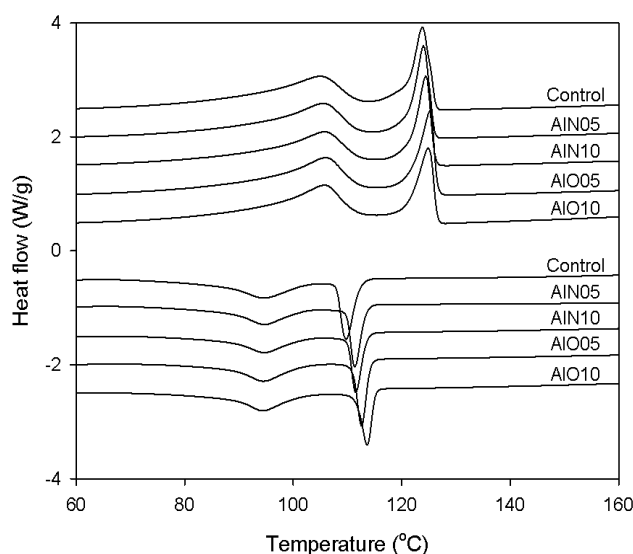
Fig. 4 (top) shows DSC melting data, from which it is evident that all systems display two broad melting peaks, at 105 ℃ and 124 ℃ (LDPE and HDPE respectively [38]). The total enthalpy is ~110 J/g for the control sample, falling in the nanocomposites to ~100 J/g, due to the proportion of included filler; the melting points do not change as a result of adding the different nanofillers. On cooling at 5 K.min^{-1} (Fig. 4, bottom), the control sample displays two crystallization peaks at 110 ℃ and 95 ℃ (HDPE and LDPE respectively). Whilst the lower (LDPE) peak is always located at the same temperature, crystallization of the HDPE occurs somewhat earlier in AlO10 (up to ~114 ℃). These thermal data therefore indicate that the alumina is having a greater nucleating effect on the polyethylene than does AlN, as expected from the disrupted textures exhibited in Fig. 3 [21, 45].

B. Nanocomposite dielectric response

Fig. 5 provides a comparison of the real and imaginary permittivity of ambient conditioned samples; that is, specimens in equilibrium with the laboratory environment. The unfilled polyethylene control sample has a real relative permittivity of 2.5 and a negligible imaginary part ($<10^{-3}$)
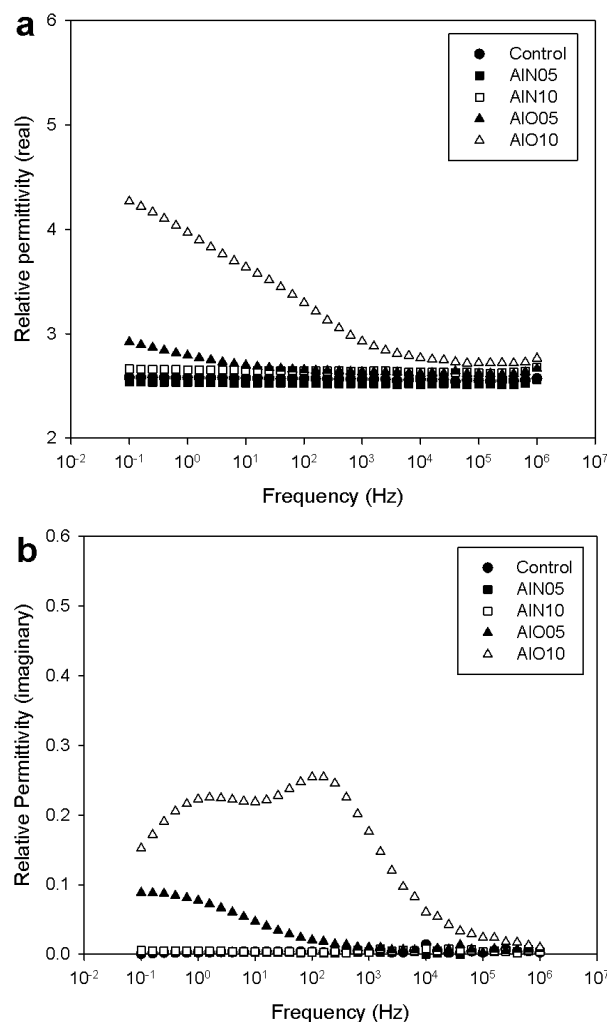
Fig. 5. Relative permittivity data obtained from samples following ambient conditioning: (a) real part; (b) imaginary part.

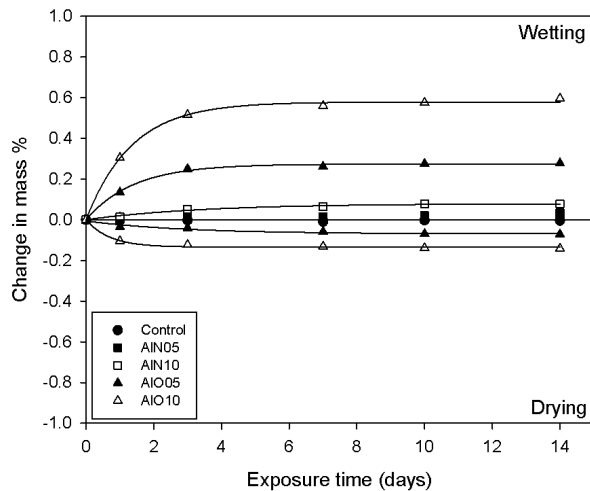Fig. 4. DSC curves from melting (top) and crystallization (bottom).

Fig. 6. Water absorption/desorption data. All data are referenced to samples exposed to laboratory conditions for 14 days.

throughout the frequency range studied here. Whilst AlN05 and AlN10 both show no differences compared with the control sample, AlO05 shows an increase in relative permittivity (Fig. 5a) and a relaxation (Fig. 5b) at low frequencies. Low frequency relaxation processes can be associated with pseudo-DC conduction and the Maxwell-Wagner effect, which is associated with the trapping of charges either at internal boundaries within materials or at the external electrodes that contact the sample [46]. Here, nanoparticle/matrix interfaces are of considerable importance in this respect and previous studies of nanocomposites have demonstrated that interfacial accumulation of water molecules can be a major contributing factor to the observed low frequency dielectric response [7, 45, 47]. In contrast, AlO10 shows two mid frequency relaxation peaks (Fig. 5b) and a strong uplift in relative permittivity below 1 kHz (Fig. 5a). In other related work [21, 48, 49], such mid frequency relaxation behavior has been attributed to water absorbed at the nanoparticle interfaces. Compared to analogous silica-based systems [37, 38], the major relaxation frequency here is much lower ~250 Hz, indicating a significantly reduced mobility of the water, as discussed in detail elsewhere [18-21].

C. Water absorption and desorption

Fig. 6 shows the measured water content relative to ambient conditioned samples with asymptotic fitted lines. The control sample is unaffected by conditioning whereas the various nanocomposites approach constant mass after 7 days. In the aluminum nitride based composites, negligible water is lost on vacuum drying (<0.01 %), indicating that this system absorbs little water on exposure to the ambient laboratory environment. This is consistent with the TGA results presented above. However, during immersion in water, AlN10 displays a small increase in mass, indicating the absorption of a small amount of water (~0.1 %). Furthermore, Fig. 5 shows that in the absence of adsorbed water, the dielectric properties of the nanocomposite are essentially the same as those of the host polymer. Whilst this general behavior is in line with that of the silicon nitride based nanocomposites [38], a far lower

water absorption is evident here. This reinforces the critical nature of the precise nanoparticle surface chemistry in determining how the material system interacts with its environment and how small changes in the local concentration of absorbed moieties can lead to marked changes in bulk dielectric properties.

In the alumina samples, it is possible to lose some 0.2 % or gain some 0.6 %, by mass, of water indicating that these materials, when stored under ambient conditions are in some intermediate state of hydration – again in agreement with the TGA data. This also conforms with previous work on silica [21, 37, 38], albeit that here the capacity to absorb water is less, presumably reflecting a reduced concentration of surface hydroxyl groups in alumina [50]. Accordingly, the resulting changes in the dielectric response relative to the host polymer (Fig. 5) are much less extreme than those exhibited by analogous silica nanocomposites [38].

D. Effect of water absorption on dielectric response

Conditioning has no effect on the control sample, which is not surprising since this sample does not absorb any appreciable water (see Fig. 5). Similarly, as indicated in Fig. 5, AlN05 is unaffected by conditioning, so data are not shown here. Figs. 7a and 7b show the effect of conditioning on the dielectric response of AlN10; in accordance with its very low water uptake (see Fig. 6), the real permittivity (Fig. 7a) is hardly affected by conditioning and, even after immersion in water, only a slight uplift in imaginary permittivity at low frequencies is evident (Fig. 7b), indicating the minimal formation of an interfacial hydration layer [48]. Figs. 7c to 7f show data obtained from AlO05 and AlO10. Drying for 14 days in vacuum eliminates the additional permittivity contribution in AlO05 (Fig. 7c) and reduces it significantly in AlO10 (Fig. 7e), whilst progressively increasing the water content results in increased real permittivity at low frequencies (Figs. 7c and 7e) and the displacement of water-related relaxation peaks to progressively higher frequencies (Figs. 7d and 7f). A qualitatively comparable shift in relaxation peak to higher frequencies with increasing water content has been reported in analogous silica systems [21, 37, 48] and is interpreted as indicating increasing mobility of water moieties at nanoparticle/matrix interfaces. However, compared to similar silica-based nanocomposites [38], the relaxation peaks observed here are much weaker, in accordance with the lower absorbed water content. Thus, there are significant advantages in using alumina or, better still, aluminum nitride in place of silica in nanodielectric applications, both in terms of reducing the propensity of the system to absorb water and, potentially, as a route to increased thermal conductivity.

E. Water content and electrical conductivity

Fig. 8a shows DC electrical conductivity values measured for each nanocomposite system, plus the unfilled control, as a function of applied field, following ambient conditioning. Compared with the unfilled control, only AlO10 shows a significantly increased conductivity, which is field dependent as reported for silica [38]; we suggest that the increased water
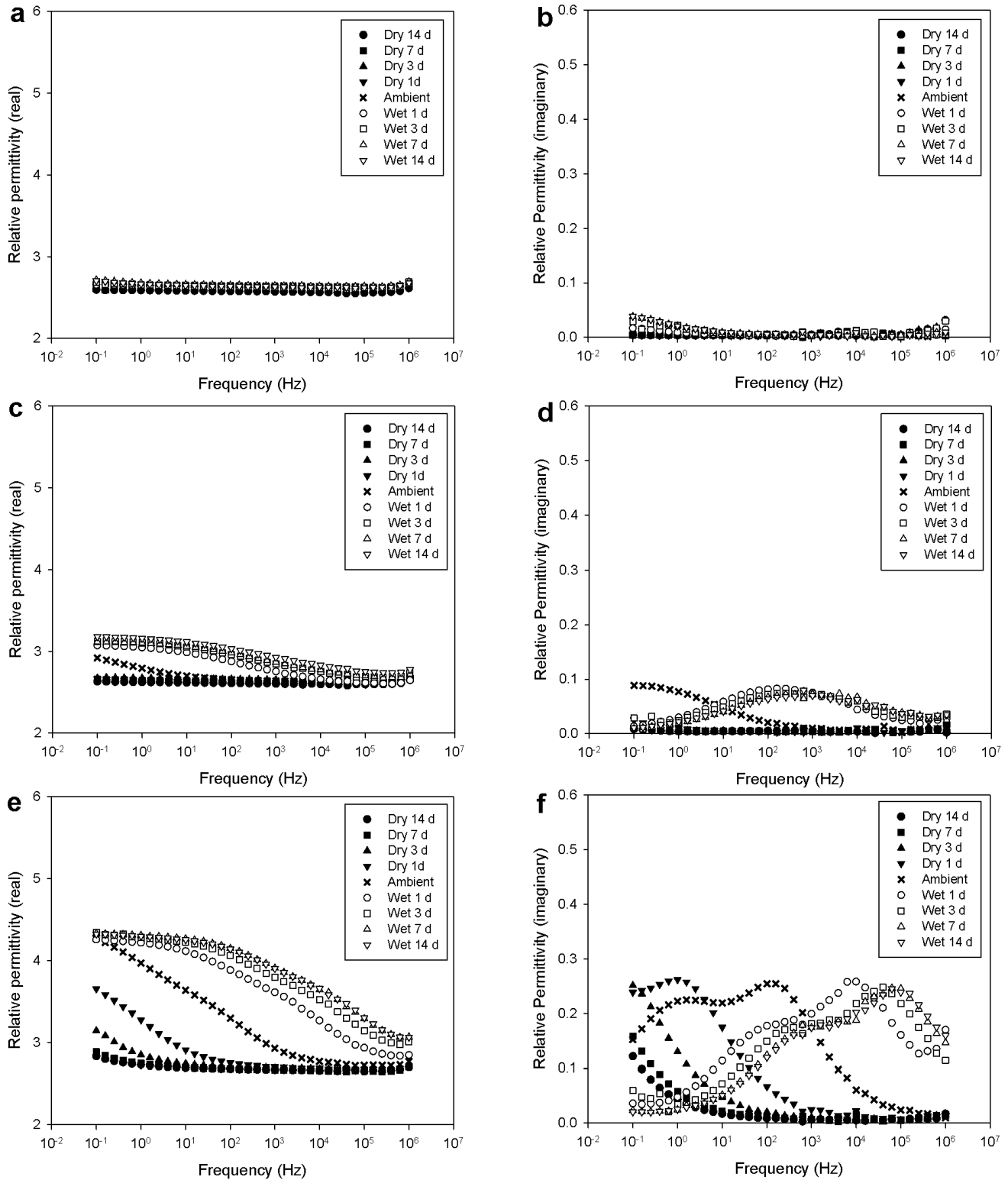
Fig. 7. Permittivity measurements: (a) AlN10 real; (b) AlN10 imaginary; (c) AlO05 real; (d) AlO05 imaginary; (e) AlO10 real;, (f) AlO10 imaginary.

content of this system is responsible [23]. After dry conditioning (Fig. 8b), this additional conductivity is largely eliminated although, as in the dielectric loss data, some contribution remains. It is suggested that this increase is either due to a retained, tightly bound hydration layer [48], or is directly associated with the presence of the nanofiller (i.e. Maxwell Wagner interfacial polarization effects).

While the nitride based composites are unaffected by wet

conditioning (Fig. 8c), a finding that is consistent with the water uptake data and dielectric spectroscopy, the alumina composites show a large increase in conductivity, which is again consistent with their increased dielectric loss and significant water uptake. Increased conductivity in nanocomposites relative to unfilled samples has been reported in other studies [23, 51] but, here, the effect is limited to only the alumina samples; i.e. those where the nanoparticle surface
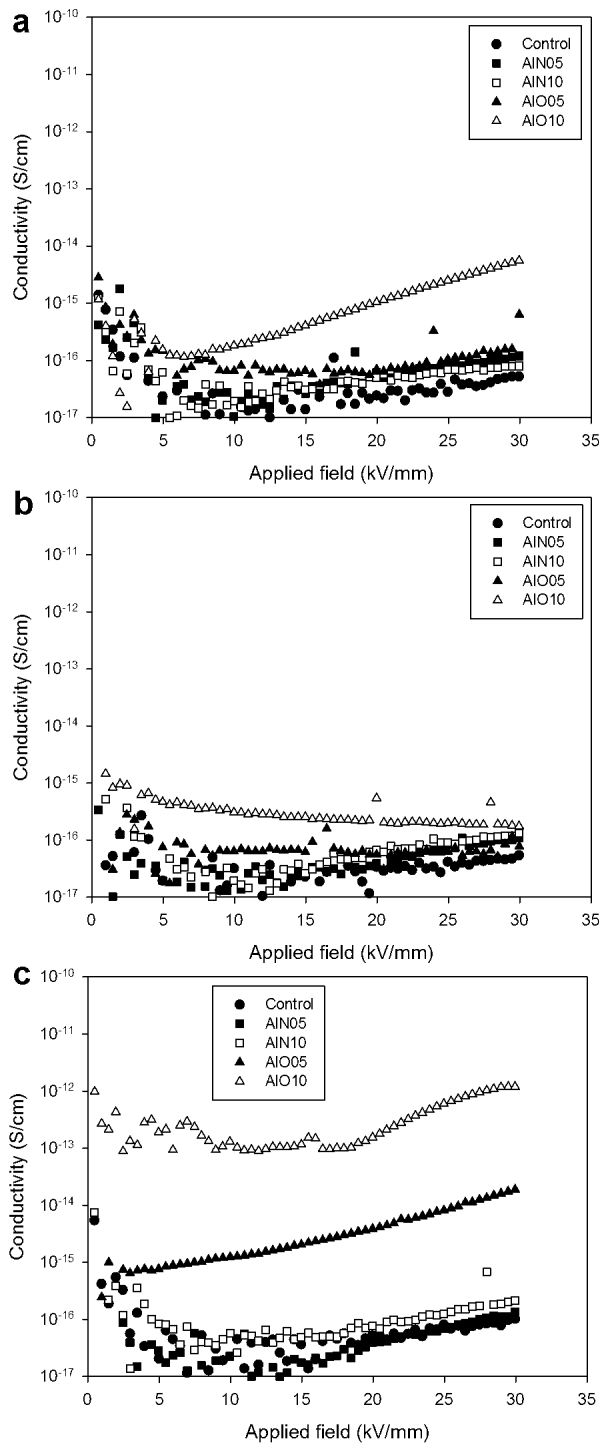
Fig. 8. Electrical conductivity measurements following: (a) ambient conditioning; (b) dry conditioning; (c) wet conditioning.

chemistry means that they are capable of absorbing significant water. For example, a strong field dependence of conductivity in silica/epoxy composites has been reported elsewhere and is consistent with a field assisted Schottky injection process [52]. We would therefore suggest that a similar process is operative here in wet conditioned samples, and is mediated by included water (including hydrated ions), which provide an additional ionic contribution to the steady state conduction current.

IV. DISCUSSION AND CONCLUSIONS

Four nanocomposites, two containing alumina and two containing aluminium nitride, were studied along with a control sample containing no nanofiller. Technologically, dielectrics will be exposed to environmental water in many application areas and, in addition, previous work has demonstrated the value of water molecules as a local dielectric probe. Consequently, the effect of conditioning (i.e. water absorption/desorption) were explored. The results described above can be summarized as follows:

- Material characterization by DSC and SEM demonstrated that all the systems considered here are structurally comparable, with no major variations in either the matrix polymer or the nanoparticle dispersion being seen. The major difference between the different nanofillers being that the aluminum nitride was composed of single particles with variable sizes whereas, in the alumina, the observed larger structures were a result of nanoparticle agglomeration.
- TGA, dielectric spectroscopy and electrical conductivity all presented a totally consistent picture concerning the different propensity of alumina and aluminium nitride to interact with water; effects that result from the different surface chemistry of the two systems.
- Electrically, the presence of water plays a dominant role in determining both the dielectric response and charge transport behavior of the systems considered here.

Our previous comparative study of silica and silicon nitride [38], whilst revealing comparable effects to those reported here was, nevertheless, adversely affected by two complicating factors: first, the nanofiller dispersion states in the silica and silicon nitride-based nanofillers were very different; second, the tendency for silicon nitride to form an oxynitride surface layer renders it much more similar to silica than might be assumed based on the bulk chemistry. The work reported here suffers from neither of these issues, lending significantly more weight to the general conclusions that can therefore be drawn.

A dominant feature of the nanodielectrics literature is variability of behavior in nominally comparable systems and we suggest that the above results, obtained from comparable samples, prepared and tested in an identical manner, supports the assertion that much of this variability may be associated with a lack of appreciation of the critical role played by low concentrations of labile species that become adsorbed onto nanoparticle surfaces. The corollary of this is that nanoparticle interfacial chemistry and the effect of this on molecular polarization effects, charge transport dynamics, etc., exert a major influence on the bulk electrical properties of nanodielectrics – a proposition that is very different from conventional ideas of property changes derived from the existence of structurally distinct interphase zones. Indeed, our work provides an additional explanation for the mechanisms by which silane functionalization of nanoparticle surfaces

leads to nanodielectrics with enhanced electrical properties. In addition to inducing favorable interactions with the matrix polymer, the process also, indirectly, has beneficial consequences through the consumption of surface hydroxyl groups. This is not to say that nanoparticle matrix interactions are of no consequence or that interphase zones do not form but, rather, that such effects do not constitute the whole story where electrical characteristics are concerned.

Finally, some comment concerning the technological implications of the work described here is warranted. Interactions with water constitute a ubiquitous feature of the environmental exposure of materials. As such, if nanodielectrics are ever to be exploited in anything other than niche applications, a key factor will be understanding (a) the mechanisms by which they interact with water and (b) the consequences of this for bulk properties. The work reported here demonstrates the importance of such effects and reveals how these can be mitigated through control of nanoparticle surface chemistry.

REFERENCES

[1] Q. T. Nguyen, D. G. Baird, "Preparation of Polymer–Clay Nanocomposites and Their Properties", Adv. Polym. Tech., vol. 25, no. 4, pp. 270–285, Win. 2006.

[2] T. J. Lewis, "Nanometric Dielectrics", IEEE Trans. Diel. Electr. Insul. vol. 1, no. 5, pp. 812-825, Oct. 1994.

[3] G. C. Stevens, A. S. Vaughan, "Nanodielectrics and their role in power transmission applications" in Electricity Transmission, Distribution and Storage Systems, Z. Melhem (ed.), Woodhead Publishing, issue 38, pp. 206-241, 2013.

[4] P. Gonon, A. Sylvestre, J. Teysseyre, C. Prior, "Combined Effects of Humidity and Thermal Stress on the Dielectric Properties of Epoxy-Silica Composites", Mater. Sci. Eng. B, vol. 83, no. 1-3, pp. 158–164, Jun. 2001.

[5] I. Rytöluoto, K. Lahti, M. Karttunen, M. Koponen, S. Virtanen, M. Pettersson, "Large-area Dielectric Breakdown Performance of Polymer Films – Part II: Interdependence of Filler Content, Processing and Breakdown Performance in Polypropylene-Silica Nanocomposites", IEEE Trans. Diel, Electr. Insul., vol. 22, no. 4, pp. 2196-2206, Aug. 2015.

[6] X. Huang, P. Jiang, "Core–Shell Structured High-k Polymer Nanocomposites for Energy Storage and Dielectric Applications", Adv. Mater., vol. 27, no. 3, pp: 546-554, Jan. 2015.

[7] T. Tanaka, "Dielectric nanocomposites with insulating properties", IEEE Trans. Diel. Electr. Insul., vol. 12, no. 5, pp. 914-928, Oct. 2005.

[8] R. C. Smith, C. Liang, M. Landry, J. K. Nelson and L. S. Schadler, "The Mechanisms Leading to the Useful Electrical Properties of Polymer Nanodielectrics", IEEE Trans. Diel. and Electr. Insul., vol. 15, no. 1, pp. 187-196, Feb. 2008.

[9] M. G. Danikas, T. Tanaka, "Nanocomposites—A Review of Electrical Treeing and Breakdown", IEEE Electr. Insul. Mag., vol. 25, no. 4, pp. 19-25, Jul-Aug. 2009.

[10] Shengtao Li, Guilai Yin, G. Chen, Jianying Li, Suna Bai, Lisheng Zhong, Yunxia Zhang , and Qingquan Lei, "Short-term Breakdown and Long-term Failure in Nanodielectrics: A Review", IEEE Trans. Diel. Electr. Insul., vol. 17, no. 5, pp. 1523-1535, Oct. 2010.

[11] M. Roy, J. K. Nelson, R. K. MacCrone, L. S. Schadler, "Candidate Mechanisms Controlling the Electrical Characteristics of Silica/XLPE Nanodielectrics", J. Mater. Sci., vol. 42, no. 11, pp. 3789-3799, Jun. 2007.

[12] S. Singha and M. J. Thomas, "Dielectric Properties of Epoxy Nanocomposites", IEEE Trans. Diel, Electr. Insul., vol. 15, no. 1, pp. 12-23, Feb. 2008.

[13] R. F. Hill, P. H. Supancic, "Determination of the Thermal Resistance of the Polymer–Ceramic Interface of Alumina-Filled Polymer Composites", J. Am. Ceram. Soc., vol. 87, no. 10, pp. 1831-1835, Oct. 2004.

[14] P. Preetha, M. J. Thomas, "AC breakdown characteristics of epoxy nanocomposites", IEEE Trans. Diel. Electr. Insul., vol. 18, no. 5, pp. 1526 - 1534 , Oct. 2011.

[15] B. B. Johnsen, T. R. Fromyr, T. Thorvaldsen, T. Olsen, "Preparation and characterisation of epoxy/alumina nanocomposites", Comp. Interf., Vol. 20, no. 9, pp. 721-740, Dec. 2013.

[16] A. Mohanty, V. K. Srivastava, "Dielectric breakdown performance of alumina/epoxy resin nanocomposites under high voltage application", Mat. Des., vol. 47, pp. 711-716, May 2013.

[17] T. S. Ramu, H. N. Nagamani, "Alumina and Silica based Epoxy Nanocomposites for Electrical Insulation", IEEE Trans. Diel. Electr. Insul. Vol. 21, No. 1, pp. 236-243, Feb. 2014.

[18] J. Mijovic, N. Miura, S. Soni, "Local Dynamics of Adhesives in Aggressive Environment in the Pre-Damage Stage", J. Adhesion, vol. 76, no. 2, pp. 123-150, Feb. 2001.

[19] R. Comrie, S. Affrossman, D. Hayward, R. A. Pethrick, "Nondestructive Examination of Epoxy Adhesive-Bonded Structures Exposed to a Humid Environment: A Comparison of Low- and High-Frequency Dielectric Measurements, J Adhesion, Vol. 78, No. 11, pp. 967-985, Nov. 2002.

[20] D. Bertolini, M. Cassettari, G. Salvetti, "The Dielectric Relaxation Time of Supercooled Water" J. Chem. Phys., vol. 76, no. 6, pp. 3285-3290, Mar. 1982.

[21] K. Y. Lau, A.S. Vaughan, G. Chen, I. L. Hosier, A. F. Holt, "On the Dielectric Response of Silica-Based Polyethylene Nanocomposites", J. Phys. D: Appl. Phys. vol.46, no, 9, 095303, Mar. 2013.

[22] N. Jaeverberg, B. Venkatesulu, H. Edin, H. Hillborg, "Prebreakdown Current and DC Breakdown Strength of Alumina-filled Poly(ethylene-co-butyl acrylate) Nanocomposites: Part I – Breakdown Strength", IEEE Trans. Diel. Electr. Insul., vol. 21, no. 5, pp. 2127-2134 , Oct. 2014.

[23] N. Jaeverberg, B. Venkatesulu, H. Edin, H. Hillborg, "Prebreakdown Current and DC Breakdown Strength of Alumina-filled Poly(ethylene-co-butyl acrylate) Nanocomposites: Part II – Prebreakdown Currents", IEEE Trans. Diel. Electr. Insul., vol. 21, no. 5, pp. 2135-2145, Oct. 2014.

[24] X. Wu, P. Jiang Y. Zhou J. Yu, F. Zhang, L. Dong, Y. Yin, "Influence of Alumina Content and Thermal Treatment on the Thermal Conductivity of UPE/Al2O3 Composite", J. Appl. Polym. Sci., vol. 131, no. 15, Art. No. 40528, Aug. 2014.

[25] S. Choi, J. Kim, "Thermal conductivity of epoxy composites with a binary-particle system of aluminum oxide and aluminum nitride fillers", Composites Part B: Engineering, vol. 51, pp. 140-147, Aug. 2013.

[26] S. Mallakpour, F. Khadem, "Recent development in the synthesis of polymer nanocomposites based on nano-alumina", Prog. Polym. Sci. Vol. 51, pp. 74-93, Dec. 2015.

[27] J. A. Pilgrim, P. L. Lewin, A. S. Vaughan, "Quantifying the Operational Benefits of New HV Cable Systems in terms of Dielectric Design Parameters", In Conf. Rec. 2012 IEEE Intern. Symp. Electr. Insul., San Juan, Puerto Rico, 2012 pp. 261-265.

[28] J. J. Park, "Dielectric Properties of Epoxy/Micro-sized Alumina Composite and of Epoxy/Micro-sized/Nano-sized Alumina Composite", Trans. Electr. Electro. Mat., Vol. 16, no. 6, pp. 338 – 341, Dec. 2015.

[29] J. J. Park, S. S. Shin, C. Y. Yoon, J. Y. Lee, J. E. Park, "Electrical and Mechanical Properties of Epoxy/Micro-sized Alumina Composite and the Effect of Nano-sized Alumina on Those Properties", IEEE Trans. Electr. Electro. Mat., Vol. 16, no. 5, pp. 260-263, Oct. 2015.

[30] Y. Xu, D. D. L. Chung, C. Mroz, "Thermally conducting aluminium nitride polymer matrix composites", Composites Part A-Appl. Sci. Manuf., vol. 32, no. 12, pp. 1749-1757, Dec. 2001

[31] E-S. Lee, S-M Lee, D. J. Shanefieldz, W. R. Cannon, "Enhanced Thermal Conductivity of Polymer Matrix Composite via High Solids Loading of Aluminum Nitride in Epoxy Resin", J. Am. Ceram. Soc., vol. 91, no. 4, pp. 1169-1174, Apr. 2008.

[32] S. Yu, P. Hing, X. Hu, "Thermal conductivity of polystyrene-aluminium nitride composite". Composites Part A-Appl. Sci. Manuf., vol. 33, no. 2, pp. 289-292, Feb. 2002.

[33] J. Gu, Q. Zhang, J. Dang, J. Zhang, Z. Yang, "Thermal Conductivity and Mechanical Properties of Aluminum Nitride Filled Linear Low-Density Polyethylene Composites", Polym. Engin. Sci., vol. 49, no. 5, pp. 1030-1034, May 2009.

[34] Y. Zhou, H. Wang, L. Wang, K. Yu, Z. Lin, L. He, Y. Bai, "Fabrication and characterization of aluminum nitride polymer matrix composites with high thermal conductivity and low dielectric constant for electronic packaging", Mat. Sci. Eng. B-Adv. Funct. Sol. St. Mater., vol. 177, no. 11, pp. 892-896, Jun. 2012.

[35] H. T. Chiu, T. Sukachonmakul, M. T. Kuo, Y. H. Wang, K. Wattanakul, "Surface modification of aluminium nitride by polysilazane and its polymer-derived amorphous silicon oxycarbide ceramic for the enhancement of thermal conductivity in silicone rubber composite", Appl. Surf. Sci., vol. 292, pp. 928-936, Feb. 2014.

[36] S. Diaham, E. Pizzutilo and M.-L. Locatelli, "DC Dielectric Strength of Epoxy/Si3N4 Nanocomposites", In Proc. Inter. Conf. Diel., Montpellier, France, 2016, pp. 72-75.

[37] I. L. Hosier, M. Praeger, A. F. Holt, A. S. Vaughan, S. G. Swingler, "Effect of water absorption on dielectric properties of nano-silica/polyethylene composites", In Proc. 2014 IEEE Conf. Electr. Insul. Diel. Phen., Des Moines, USA, 2014, pp. 651-654.

[38] I. L. Hosier, M. Praeger, A. S. Vaughan, S. G. Swingler, "The effects of water on the dielectric properties of silicon based nanocomposites", IEEE Trans. Nanotech, vol. 16, no. 2, pp. 169-179, Mar. 2017.

[39] R. H. Olley and D. C. Bassett, "An improved permanganic etchant for polyolefins", Polymer, vol. 23, no. 12, pp. 1707-1710, Nov. 1982.

[40] E. W. Osborne, M. G. Norton, "Oxidation of aluminium nitride", J. Mat. Sci., vol. 33, no. 15, pp. 3859-3865, Aug. 1998.

[41] C. Z. Liao, S. C. Tjong, "Mechanical and Thermal Performance of High-Density Polyethylene/Alumina Nanocomposites", J. Macromol. Sci. B-Phys., vol. 52, no. 6, pp. 812-825, May 2013.

[42] J. W. Gu, Q. Y. Zhang, J. Dang, J. P. Zhang, Z. Y. Yang, "Thermal Conductivity and Mechanical Properties of Aluminum Nitride Filled Linear Low-Density Polyethylene Composites", Polym. Eng. Sci., vol. 49, no. 5, pp. 1030-1034, May 2009.

[43] R. Fu, K. Chen, S. Agathopoulos, J. M. F. Ferreira, "Factors which Affect the Morphology of AlN Particles Made by Self-Propagating High-Temperature Synthesis (SHS)", J Cryst. Growth", vol. 296, no. 1, pp. 97–103, Oct. 2006.

[44] C. Chazelas, J.F. Coudert, J. Jarrige, P. Fauchais "Synthesis of Ultra Fine Particles by Plasma Transferred Arc: Influence of Anode Material on Particle Properties", J. Eur. Ceram. Soc., vol. 26, no. 16, pp. 3499-3507, Dec. 2006

[45] D. M. Panaitescu, Z. Vuluga, P. V. Notingher, C. Nicolae, "The Effect of Poly[styrene-b-(ethylene-co-butylene)-b-styrene] on Dielectric, Thermal, and Morphological Characteristics of Polypropylene/Silica Nanocomposites", Polym. Engin. Sci., vol. 53, no. 10, pp. 2081-2092, Oct. 2013.

[46] A. Schönhals, F. Kremer, "Analysis of Dielectric Spectra", in Broadband Dielectric Spectroscopy, F. Kremer, A. Schönhals (eds.), Springer-Verlag Berlin Heidelberg, pp. 59-98, 2003.

[47] H. Couderc, M. Frechette, E. David, "Fabrication and Dielectric Properties of Polypropylene/Silica Nanocomposites", In Proc. 2015 IEEE Electr. Insul. Conf., Seattle WA, USA, 2015, pp. 329-332.

[48] L. Hui, L. S. Schadler, J. K. Nelson, "The Influence of Moisture on the Electrical Properties of Crosslinked Polyethylene/Silica Nanocomposites", IEEE Trans. Diel. Electr. Insul., vol. 20, no. 2, pp. 641 – 653, Apr. 2013.

[49] M. Roy, J. K. Nelson, R.K. MacCrone, L.S. Schadler, C.W. Reed, R. Keefe and W. Zenger, "Polymer Nanocomposite Dielectrics – The Role of the Interface", IEEE Trans. Diel. Electr. Insul., vol. 12, no. 4, pp. 629-643, Aug. 2005.

[50] Y. Rozita, R. Brydson, A. J. Scott, "An investigation of commercial gamma-Al2O3 nanoparticles", J. Phys. Conf. Ser., vol. 241, Aug. 2010, Art. No. 012096.

[51] S. L. Abd-El Messieh, N. N. Rozik, "Dielectric and Morphological Studies on Polyester/Nanosilica Fume Composites", J. Appl. Polym. Sci., vol. 122, no. 1, pp. 714–721, Oct. 2011.

[52] J. Castellon, H. N. Nguyen, S. Agnel, A. Toureille, M. Fréchette, S. Savoie, A. Krivda and L.E. Schmidt, "Electrical Properties Analysis of Micro and Nano Composite Epoxy Resin Materials", IEEE Trans. Diel. Electr. Insul., vol. 18, no. 3, pp. 651-658, Jun. 2011.
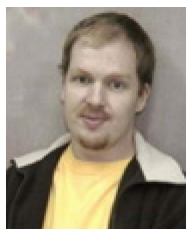
Ian Hosier received the B.Sc. degree in physics and the Ph.D. degree in polymer physics from The University of Reading, UK. He then went on with postdoctoral research at the same university, which involved extensive collaborations with institutions in Germany and Japan. In 2001 he accepted a placement at Florida State University in the USA looking at atomic force microscopy of semi-crystalline polymer blends. In 2003 he returned to the UK to take a research post at the University of Southampton looking at the aging behavior of a variety of solid and liquid insulation materials. Research interests include dielectrics, ageing, microscopy and polymer morphology.

Matthew Praeger has an M.Phys degree in Physics with Laser Science and received a Ph.D for Laser Generation of X-rays; both were awarded by the University of Southampton. He subsequently worked at the Optoelectronics Research Centre on laser beam characterization but then shifted focus to applications, developing microfluidic and electrohydrodynamic devices. Since moving to the Electrical and Electronic Engineering group he has pursued interests in electrical phenomena such as dielectrophoresis and in nanocomposite materials for dielectric applications.

Alun Vaughan (SM'07) has a B.Sc. degree in chemical physics and a Ph.D. degree in polymer physics. After working at the UK's Central Electricity Research Laboratories and spending a period as an academic at The University of Reading, he is now Professor of Dielectric Materials and Head of the Electronics and Electrical Engineering research group at the University of Southampton. He is a former chair of The Dielectrics Group of the Institute of Physics, a Fellow of the Institute of Physics, a Fellow of the IET and in 2016 delivered the IEEE DEIS Eric O. Forster memorial lecture.

Steve Swingler received the B.A. and Ph.D. degrees in physics from the University of Lancaster. In 1976 he was appointed Pirelli Postdoctoral Research Fellow at Southampton University, investigating dielectrics for superconducting and extruded dc cables. He joined the Central Electricity Research Laboratories at Leatherhead in 1979 working mainly on novel cable systems and insulating materials. In 1990 he transferred to the National Grid Company, becoming Cables Manager and then Company Undergrounding Adviser. In 2003 he joined the School of Electronics & Computer Science at Southampton University as Professor in Transmission Asset Engineering. He is the UK Member of CIGRE Study Committee B1 (High Voltage Cables).